THE GEOLOGICAL SOCIETY OF AMERICA®

Equable end Mesoproterozoic climate in the absence of high CO_2

Richard P. Fiorella* and Nathan D. Sheldon
Department of Earth and Environmental Sciences, University of Michigan, Ann Arbor, Michigan 48109, USA

ABSTRACT

The Proterozoic Eon (2500–542 Ma) appears to have been a warm period bookended by glaciations, despite a 5%–18% reduction in solar output compared to modern during this interval. Radiative-convective climate models suggest that glaciation could have been avoided if pCO_2 were 30–300× preindustrial atmospheric levels (PIAL, 280 ppmv). Constraints from late Mesoproterozoic (ca. 1.2–1.0 Ga) microfossil calcification sheaths and paleosol mass balance, however, suggest that pCO_2 may have been no higher than 10× PIAL. In the lower oxygen Mesoproterozoic atmosphere, an increased CH_4 flux from methanogenic bacteria may have contributed additional greenhouse warming. We use a fully coupled atmosphere-ocean general circulation model (the U.S. National Center for Atmospheric Research Community Earth System Model, CESM) to test whether these pCO_2 constraints are consistent with the absence of widespread glaciation inferred from the geologic record. We vary pCO_2 and pCH_4 between 1400 and 2800 ppmv and 3.5 and 140 ppmv, respectively, using a reconstructed 1.0 Ga paleogeography and solar output reduced by 9%. Our simulations suggest that ice-free conditions can be maintained at 10× PIAL CO_2 when CH_4 is 140 ppmv. When CH_4 is lowered to 28 ppmv at 10× PIAL CO_2, or if pCO_2 is lowered to 5× PIAL, permanent land snow cover at high and middle latitudes suggests that glaciation would be more extensive than preindustrial conditions, but with warm tropical regions. Global glaciation occurs if pCO_2 is reduced below 5× PIAL. Overall, our simulations suggest that an ice-free climate for the Mesoproterozoic (1.6–1.0 Ga) is consistent with the relatively low pCO_2 implied from proxies if CH_4 or other greenhouse gas concentrations were sufficiently elevated.

INTRODUCTION

Earth received 5%–18% less energy from the sun during the Proterozoic Eon (2500–542 Ma) (Gough, 1981). Despite this decreased solar luminosity, geologic evidence suggests a warm climate for the majority of the Proterozoic (Table DR1 in the GSA Data Repository[1]), bookended by two major glaciations ca. 2.4 Ga and ca. 0.8–0.6 Ga (Hoffman, 1998; Kirschvink et al., 2000). Elevated greenhouse gas concentrations have been invoked to explain the absence of glaciers from 2.4–0.8 Ga. For example, one-dimensional (1-D) climate models suggest that pCO_2 levels of 30–300× preindustrial atmospheric levels (PIAL, 280 ppm CO_2) are required to explain the lack of glaciation (e.g., Kasting, 1987; Roberson et al., 2011). However, recent proxy reconstructions of pCO_2 levels ca. 1.0 Ga based on paleosol mass balance (Mitchell and Sheldon, 2010; Sheldon, 2013) and microfossil calcification sheaths (Kah and Riding, 2007) limit pCO_2 to ~10× PIAL, much lower than the >25× PIAL calculated from Paleoproterozoic paleosols (e.g., Sheldon, 2006; Kanzaki and Murakami, 2015) and the 30–300 PIAL required by radiative-convective models to avoid glaciation. The lower pCO_2 levels implied by geologic proxies than by 1-D climate models, and the long-term drawdown in pCO_2 across the Proterozoic inferred by paleosol mass balance, raise the question of whether 10× PIAL CO_2 at 1.2–1.0 Ga is consistent with the absence of glaciation when dynamic feedbacks are considered in a 3-D climate model.

We use a fully coupled global climate model (GCM) to estimate the glacial extent associated with a 9% reduction to the modern solar constant and $pCO_2 \leq 10\times$ PIAL. To our knowledge, these are the first simulations of paleoclimate at 1.0 Ga using a fully coupled GCM. We also vary the atmospheric methane concentration, as methane produced by methanogenic bacteria could have accumulated to much higher than modern levels if the flux were greater, or if oxygen levels were low and the ocean were sulfate poor (e.g., Pavlov et al., 2003). Oxygen levels at 1.0 Ga were likely ≤0.01 PIAL (Kump, 2008), and may have been lower by as much as three orders of magnitude (Lyons et al., 2014). From these simulations, we identify greenhouse gas inventories consistent with climate states lacking permanent ice cover; climate states that have the potential for high- and mid-latitude glaciation; or climate states that suggest complete, planetary glaciation.

METHODS

The U.S. National Center for Atmospheric Research Community Earth System Model (CESM v.1.2), a state-of-the-science climate model with prognostic atmosphere (CAM4, Community Atmosphere Model, version 4), ocean (POP2, Parallel Ocean Program version 2), land (CLM4, Community Land Model version 4.0), and sea ice (CICE4, Los Alamos Sea Ice Model, version 4) components linked by a coupler (Hurrell et al., 2013), was used to simulate end Mesoproterozoic climate. Trace gases such as CO_2 and CH_4 are well mixed in the troposphere (Neale et al., 2010). The atmosphere and land components used resolution grid T31 (~3.75°), while the ocean and sea ice models are ~3°. Boundary conditions were set to match hypothesized Mesoproterozoic conditions. Solar luminosity was reduced by 9% (Gough, 1981). We used a paleogeographic map for 1.0 Ga (Li et al., 2008); POP2 requires land at both poles, so a small island representing ~1% of the global land mass was added to the north geographic pole (Fig. 1A). Mean topography (bathymetry) was 500 m (4000 m). Land plants were removed because they had not yet evolved. Ocean, sea ice, and snow albedos were set to model defaults; land surface albedo varies with increasing soil water content from 0.08 and 0.04 in visible wavelengths, and 0.16 and 0.08 in the near-infrared, typical of basalt (Hartmann, 1994). We calculated an aerosol climatology accounting for paleogeographic changes (after Heavens et al., 2012). Additional details about albedo specifications are given in the Data Repository.

Three suites of simulations were performed (Table 1; Tables DR2 and DR3). First, six simulations with differing CO_2 and CH_4 concentrations consistent with late Mesoproterozoic proxy records were carried out using a fully dynamic ocean. The CO_2 concentrations were specified as either 1400 or 2800 ppmv (i.e., 5× or 10× PIAL). CH_4 concentrations were set to 3.5 or 70 ppmv (1:400 or 1:20 CH_4:CO_2 ratio) when CO_2 was set to 1400 ppmv (cases G1 and G2; Table 1), and 28 and 140 ppmv (1:100 or 1:20 CH_4:CO_2 ratio) when CO_2 was set to 2800 ppmv (cases G3 and G4; Table 1). While CH_4:CO_2 ratios of 1:100 or 1:20 are significantly higher than the modern ratio of ~1:400, they are too low to form organic aerosol hazes that may counteract greenhouse warming (Trainer et al., 2006; Domagal-Goldman et al., 2008). To test the sensitivity of these results to paleogeographic uncertainty (e.g., Fiorella and Poulsen, 2013), simulations G1

*Current address: Department of Geology and Geophysics, University of Utah, 115 S. 1460 E., 383 Frederick A Sutton Building, Salt Lake City, Utah 84112, USA; E-mail: rich.fiorella@utah.edu.

[1]GSA Data Repository item 2017060, Late Mesoproterozoic sedimentary sections and GCM sensitivity setup and extended results, is available online at www.geosociety.org/datarepository/2017 or on request from editing@geosociety.org.

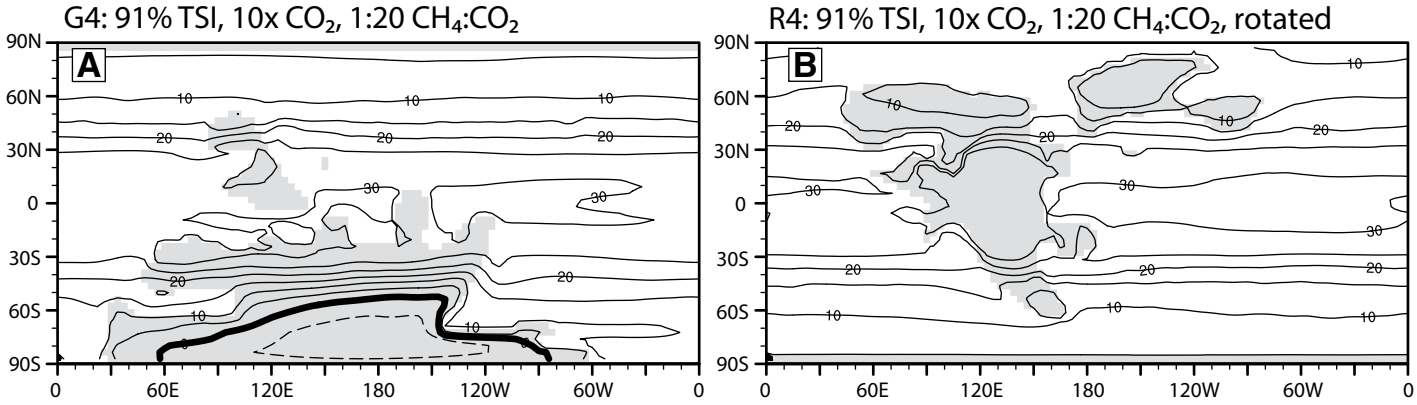

Figure 1. A: Mean annual surface temperatures for the Li et al. (2008) continental reconstruction (case G4). Continents are shaded in gray. The mean annual freezing isotherm (0 °C) is drawn as a heavy line; positive temperature contours are shown as solid thin lines; negative temperature contours are shown as dashed lines. B: A 90° rotation of this configuration (case R4). The greenhouse gas forcings in these two simulations are identical.

TABLE 1. SUMMARY OF COUPLED GLOBAL CLIMATE MODEL SIMULATIONS

Case name	CO_2 (ppmv)	CH_4 (ppmv)	Global mean *T* (°C)	Tropical mean *T* (°C)	Mean *T* <0 °C (land, %)	Permanent snow cover (land, %)	Mean sea ice latitude	TOA albedo	Surface albedo	Cloud cover (%)
Li et al.(2008) paleogeography at 1.0 Ga										
G1	1400	3.5	4.3	19.4	48	53	51.3	0.37	0.23	59
G2	1400	70	13.5	23.9	35	33	69.8	0.34	0.14	62
G3	2800	28	17.4	26.0	27	15	79.5	0.33	0.11	62
G4	2800	140	21.4	28.7	14	0	90	0.32	0.09	62
Li et al. (2008) paleogeography at 1.0 Ga, rotated 90°										
R1	1400	3.5	3.4	18.3	40	45	49	0.37	0.24	59
R4	2800	140	22.3	29.6	0	0	90	0.31	0.08	63

Note: T—temperature; TOA—top of atmosphere.

and G4 were repeated using a rotated continental configuration (cases R1 and R4; Table 1), which changed the continental distribution from predominantly polar to more tropical (Fig. 1B). These simulations were integrated for at least 2000 model years until equilibrium was reached, and the results here are averages of the past 30 yr of model integration.

We extended our fully coupled simulations with two suites of sensitivity tests where the dynamic ocean was replaced with a mixed-layer ocean, which permitted testing of a wider range of conditions. In the first suite, simulations G1–G4, R1, and R4 were extended with atmospheric aerosols removed (noaero), prescribed ocean heat transport set to zero, or the land albedo increased (sc1 and sc11; Table DR2). In the second, we paired pCO_2 of 10×, 5×, and 1× PIAL with CH_4:CO_2 ratios of 1:20, 1:100, 1:400, and 0 (Table DR3) using the climatological ocean heat transport from simulation G1. Additional details of the model setup for these sensitivity suites are provided in the Data Repository.

RESULTS

Global and tropical mean surface temperatures range from 4.2 °C to 21.4 °C and 19.4 °C to 28.7 °C for the smallest (G1; Fig. 1A) and largest (G4), greenhouse gas concentrations for simulations using the Li et al. (2008) 1.0 Ga paleogeography (Table 1; Fig. 1A). Despite warm tropics in all four simulations, substantial differences in high- and mid-latitude temperatures are observed. The warmest simulation (G4) has no permanent sea ice or continental snow cover; in contrast, simulation G1 has a mean sea ice front at 51.3°, 53% of the continental land surface has permanent snow cover, and mean land temperatures >0 °C are restricted to the tropics (Fig. 1A). Continental rotation has little effect on global or tropical mean temperatures, permanent snow cover, or mean sea ice latitude (Table 1). R1 exhibits global and tropical temperatures ~1 °C lower than G1 and a ~2° expansion of sea ice, while R4 exhibits global and tropical temperatures ~1 °C higher than G4 and no change in sea ice, despite equal greenhouse gas concentrations in these simulation pairs (Fig. 1; Table 1). However, global land temperatures increase by ~3–5 °C as the continental rotation shifts landmasses into the middle to low latitudes, promoting a reduction in the area of land with mean annual temperatures below freezing (Table 1). The percentage of land with permanent snow cover decreases in R1 relative to G1, and is 0% for both R4 and G4 (Table 1). Global glaciation is not observed, and the highest greenhouse gas inventories examined are free of permanent snow cover and sea ice.

Removing aerosols from the model (noaero; Table DR2) had a small impact on global temperatures (increased by <1.5 °C). Removing aerosols was associated with an increase in atmospheric humidity and resultant stronger greenhouse forcing. In contrast, setting the ocean heat transport to zero everywhere (noht; Table DR2) reduced global average temperatures by >14 °C. This change in ocean heat transport does not change the total radiative forcing in the model, but instead prevents the ocean from redistributing energy from low to high latitudes (e.g., Poulsen et al., 2001). As a result, sea ice expands equatorward, with the largest impact occurring when greenhouse gas forcing is lower (Table DR2). Increasing the land albedo to 0.36 (sc1; Table DR2) reduced global temperatures by >10 °C in the Li et al. (2008) configuration, when land was concentrated at high latitudes, but by <10 °C when land was rotated into low latitudes (Table DR2). In the former cases, increasing the albedo of high-latitude land preferentially cools the high latitudes and expands the land area conducive to permanent snow cover (Table DR2).

Our sensitivity analysis using wider ranges of pCO_2 and pCH_4 demonstrates that regardless of the pCH_4 levels, 5× and 10× PIAL CO_2 levels are sufficient to avoid global-scale glaciation, but 1× PIAL CO_2 levels are not

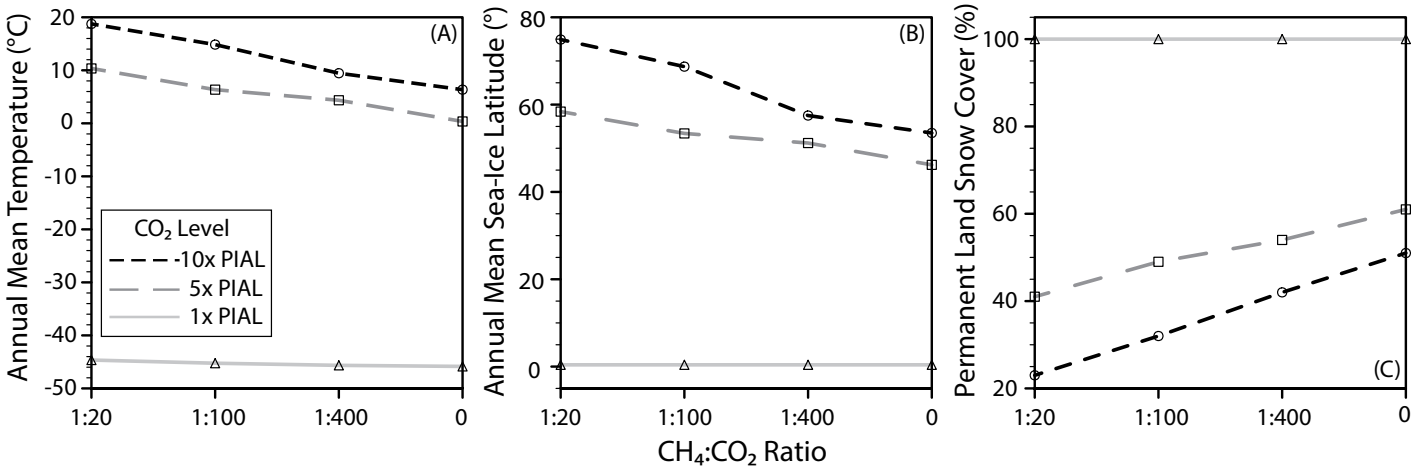

Figure 2. Sensitivity of results to an expanded range of greenhouse forcing: 10× (black, short dash), 5× (dark gray, long dash), 1× (light gray, solid), and preindustrial level (PIAL) pCO_2 are paired with CH_4:CO_2 ratios of 1:20, 1:100, 1:400, and 0. A: Annual mean temperature (°C). B: Annual mean sea ice latitude (°). C: Land area possessing permanent snow cover (%).

(Fig. 2; Table DR3). At all pCH_4, global temperatures at 1× PIAL CO_2 are <–40 °C, sea ice extends to the equator, and 100% of the land surface has permanent snow cover (Fig. 2; Table DR3). In contrast, at >5× PIAL pCO_2, mean annual temperatures are >0 °C, sea ice remains poleward of ~50°, and <60% of the land area has permanent snow cover (Fig. 2; Table DR3). At >5× PIAL pCO_2, high- and mid-latitude conditions are highly sensitive to pCH_4, with higher CH_4 concentrations promoting higher global temperatures, poleward contraction of sea ice, and reduction in land snow cover.

DISCUSSION

Sedimentary evidence for widespread glaciation is absent between 2.4 and 0.8 Ga (Table DR1), leading to the inference that no ice sheets were present, or they were confined to small areas during this period. Ice-free conditions can be maintained at 1.0 Ga with pCO_2 constraints inferred from paleosol mass balance and microfossil traces if pCH_4 is sufficiently high. Perennial snow cover and sea ice are absent in simulations G4 and R4, which had pCO_2 of 2800 ppmv and pCH_4 of 140 ppmv. The other fully coupled simulations suggest that limited high- to mid-latitude glaciation can arise from a wide range of greenhouse gas inventories. In the simulations with a mixed-layer ocean model, 5× to 10× PIAL CO_2 levels are conducive to high- to mid-latitude glaciation, with snow and sea ice extent decreasing with increasing pCO_2 and pCH_4. When CO_2 is reduced to 1× PIAL, no CH_4:CO_2 ratio tested is sufficient to avoid global glaciation; other sources of warming would be required to explain the lack of glaciation at the lowest pCO_2 inferred from paleosol mass balance (Sheldon, 2013). Furthermore, we identify surface albedo and ocean heat transport as key parameters determining the extent of permanent snow cover and glaciation potential. These parameters are poorly constrained at 1.0 Ga, but largely determine high-latitude energy balance and temperature. Our estimation of glacial extent using permanent snow cover may be conservative. Glaciers and ice sheets flow from accumulation to ablation areas; permanent snow cover represents only the accumulation areas. Topography is also highly idealized in our simulations; inclusion of mountain ranges may increase glacial extent by reducing surface temperatures and increasing snowfall rates. However, many 1-D model studies have used a global mean temperature of 0 °C as a threshold for global glaciation (e.g., Kasting, 1987; Goldblatt et al., 2009), yet global mean temperatures can be <0 °C without triggering global glaciation in 3-D models (Table DR3; also Wolf and Toon, 2013; Fiorella and Poulsen, 2013), suggesting that 1-D models may overestimate the greenhouse forcing required to avoid global ice cover.

Maintaining high pCH_4 would require an elevated CH_4 flux from methanogenic bacteria or a reduced atmospheric photochemical sink. Prior estimates of the methanogenic flux from a low-oxygen, sulfidic ocean indicate that a flux ~10–20× greater than modern is reasonable, which could yield as much as ~100–300 ppmv CH_4 if pO_2 is between 0.01 and 1× PIAL (Pavlov et al., 2003). However, Mesoproterozoic O_2 may have been <0.001 PIAL (Reinhard et al., 2013; Lyons et al., 2014). Were pO_2 this low, the photolysis rate of CH_4 would have been higher due to decreased shielding of ultraviolet radiation from lower ozone concentrations (Kasting, 1987), and CH_4 fluxes would have had to be correspondingly higher to maintain atmospheric CH_4 concentrations of 100–300 ppmv. Modeling by Olson et al. (2016) suggests that efficient CH_4 coupling to SO_4^{2-} reduction in the oceans may have limited Mesoproterozoic pCH_4 to <10 ppmv; if their model is correct, then the G1 and R1 (Table 1) scenarios could be considered most likely. However, given the evidence for low pCO_2 and the dearth of evidence for mid-latitude glaciation that our simulations indicate would result from such low pCH_4 (Table DR1), higher pCH_4 scenarios (G2–G4, R4; Table 1) are more consistent with the geologic record.

If high pCH_4 could not have been sustained, what other factors may explain the apparent lack of glaciation? The Mesoproterozoic sedimentary record is sparse (Table DR1), and a large portion of the sedimentary record has likely been lost. As a result, high- to mid-latitude glaciation may have occurred without any preserved evidence. Paleogeographic reconstructions are inherently uncertain, and multiple reconstructions for 1.0 Ga exist. Concentrating land in the tropics reduces the fraction of land susceptible to glaciation; however, solving the apparent lack of glaciation at 1.0 Ga by moving continents into the tropics simply shifts the paradox elsewhere in the Proterozoic. The Mesoproterozoic atmosphere may have been different in terms of the concentrations of other greenhouse gases (e.g., N_2O), total atmospheric pressure, and cloud properties. Buick (2007) suggested that a euxinic Mesoproterozoic ocean would have promoted an increase in the N_2O flux to the atmosphere of as much as ~20-fold. N_2O has a higher warming potential than CH_4, thus modest increases in N_2O could offset substantial decreases in CH_4. For example, a 10-fold increase in N_2O from 0.3 to 3.0 ppmv would offset decreases in CH_4 from 140 ppmv to ~30 ppmv (e.g., simulations G4 and R4; Byrne and Goldblatt, 2014); prior modeling studies have considered N_2O concentrations up to 30 ppmv (Roberson et al., 2011). Second, reconstructions of Archean atmospheric density from fossil raindrops (Som et al., 2012), nitrogen isotopes (Marty et al., 2013), and basalt vesicles (Som et al., 2016) suggest a dynamic history for atmospheric density during the Precambrian. Increased atmospheric pressure would have a warming effect by broadening the absorption lines of greenhouse gases (Goldblatt et al., 2009), but recent 3-D GCM results indicate that regional changes in water vapor,

lapse rate, and cloud climate feedbacks may counteract this warming impact (Poulsen et al., 2015). Regional variability in feedback strength is not simulated in 1-D climate models. Changes in cloud properties can warm the surface through radiative changes. For example, if the concentration of cloud condensation nuclei were lower in the Mesoproterozoic, low-level clouds would rainout more efficiently and occur less frequently; this would warm the surface (Kump and Pollard, 2008).

CONCLUSIONS

Mesoproterozoic paleosols and microfossils suggest pCO_2 levels of ~10× preindustrial values or less, implying a long-term drawdown from much higher Paleoproterozoic levels. Here we used a 3-D GCM to test whether these low greenhouse gas compositions are consistent with the absence of glaciation at 1.0 Ga, despite 9% lower solar luminosity than modern. If the geologic record is strictly interpreted to indicate that the Mesoproterozoic Eon was generally ice free, our simulations indicate that 10× PIAL CO_2 combined with 140 ppmv of CH_4 is sufficient. If CH_4 is lowered to 28 ppmv at 10× PIAL CO_2, modest glaciation comparable to preindustrial or last glacial maximum conditions are obtained. Thus, the threshold for ice-free conditions with 10× PIAL can be bracketed to between 28 and 140 ppmv of CH_4. If CH_4 could not have been maintained at the levels our simulations suggest would be required to avoid development of substantial land ice, we speculate that mechanisms such as increased N_2O or changes in cloud properties, surface albedo, or atmospheric pressure could all contribute to end-Mesoproterozoic warmth. If the possibility of regional high- to mid-latitude glaciation and warm tropical latitudes can be permitted, recognizing the limited coverage of sedimentary records, a much wider range of Mesoproterozoic boundary conditions is consistent with the geologic record.

ACKNOWLEDGMENTS

Fiorella received support from National Science Foundation (NSF) Graduate Research Fellowship grant 2011094378. Sheldon received support from NSF grant 1050760. Global climate model simulations in this study were conducted on the National Center for Atmospheric Research Yellowstone supercomputer as part of awards UMIC0019 and UMIC0043. Simulation results are archived in the National Oceanic and Atmospheric Administration World Data Center for Paleoclimatology (https://www.ncdc.noaa.gov/paleo/study/20990). We thank T.W. Lyons, C. Goldblatt, S. Driese, and an anonymous reviewer for suggestions that improved this manuscript.

REFERENCES CITED

Buick, R., 2007, Did the Proterozoic "Canfield Ocean" cause a laughing gas greenhouse?: Geobiology, v. 5, p. 97–100, doi:10.1111/j.1472-4669.2007.00110.x.

Byrne, B., and Goldblatt, C., 2014, Radiative forcing at high concentrations of well-mixed greenhouse gases: Geophysical Research Letters, v. 41, p. 152–160, doi:10.1002/2013GL058456.

Domagal-Goldman, S.D., Kasting, J.F., Johnston, D.T., and Farquhar, J., 2008, Organic haze, glaciations and multiple sulfur isotopes in the Mid-Archean Era: Earth and Planetary Science Letters, v. 269, p. 29–40, doi:10.1016/j.epsl.2008.01.040.

Fiorella, R.P., and Poulsen, C.J., 2013, Dehumidification over tropical continents reduces climate sensitivity and inhibits snowball Earth initiation: Journal of Climate, v. 26, p. 9677–9695, doi:10.1175/JCLI-D-12-00820.1.

Goldblatt, C., Claire, M.W., Lenton, T.M., Matthews, A.J., Watson, A.J., and Zahnle, K.J., 2009, Nitrogen-enhanced greenhouse warming on early Earth: Nature Geoscience, v. 2, p. 891–896, doi:10.1038/ngeo692.

Gough, D.O., 1981, Solar interior structure and luminosity variations: Solar Physics, v. 74, p. 21–34, doi:10.1007/BF00151270.

Hartmann, D.L., 1994, Global physical climatology: San Diego, California, Academic Press, 411 p.

Heavens, N.G., Shields, C.A., and Mahowald, N.M., 2012, A paleogeographic approach to aerosol prescription in simulations of deep time climate: Journal of Advances in Modeling Earth Systems, v. 4, M11002, doi:10.1029/2012MS000166.

Hoffman, P.F., 1998, A Neoproterozoic Snowball Earth: Science, v. 281, p. 1342–1346, doi:10.1126/science.281.5381.1342.

Hurrell, J.W., et al., 2013, The Community Earth System Model: A framework for collaborative research: American Meteorological Society Bulletin, v. 94, p. 1339–1360, doi:10.1175/BAMS-D-12-00121.1.

Kah, L.C., and Riding, R., 2007, Mesoproterozoic carbon dioxide levels inferred from calcified cyanobacteria: Geology, v. 35, p. 799–802, doi:10.1130/G23680A.1.

Kanzaki, Y., and Murakami, T., 2015, Estimates of atmospheric CO_2 in the Neoarchean–Paleoproterozoic from paleosols: Geochimica et Cosmochimica Acta, v. 159, p. 190–219, doi:10.1016/j.gca.2015.03.011.

Kasting, J.F., 1987, Theoretical constraints on oxygen and carbon dioxide concentrations in the Precambrian atmosphere: Precambrian Research, v. 34, p. 205–229, doi:10.1016/0301-9268(87)90001-5.

Kirschvink, J.L., Gaidos, E.J., Bertani, L.E., Beukes, N.J., Gutzmer, J., Maepa, L.N., and Steinberger, R.E., 2000, Paleoproterozoic snowball Earth: Extreme climatic and geochemical global change and its biological consequences: National Academy of Sciences Proceedings, v. 97, p. 1400–1405, doi:10.1073/pnas.97.4.1400.

Kump, L.R., 2008, The rise of atmospheric oxygen: Nature, v. 451, p. 277–278, doi:10.1038/nature06587.

Kump, L.R., and Pollard, D., 2008, Amplification of Cretaceous warmth by biological cloud feedbacks: Science, v. 320, p. 195, doi:10.1126/science.1153883.

Li, Z.X., et al., 2008, Assembly, configuration, and break-up history of Rodinia: A synthesis: Precambrian Research, v. 160, p. 179–210, doi:10.1016/j.precamres.2007.04.021.

Lyons, T.W., Reinhard, C.T., and Planavsky, N.J., 2014, The rise of oxygen in Earth's early ocean and atmosphere: Nature, v. 506, p. 307–315, doi:10.1038/nature13068.

Marty, B., Zimmermann, L., Pujol, M., Burgess, R., and Philippot, P., 2013, Nitrogen isotopic composition and density of the Archean atmosphere: Science, v. 342, p. 101–104, doi:10.1126/science.1240971.

Mitchell, R.L., and Sheldon, N.D., 2010, The ~1100 Ma Sturgeon Falls paleosol revisited: Implications for Mesoproterozoic weathering environments and atmospheric CO_2 levels: Precambrian Research, v. 183, p. 738–748, doi:10.1016/j.precamres.2010.09.003.

Neale, R.B., et al., 2010, Description of the NCAR Community Atmosphere Model (CAM 4.0): National Center for Atmospheric Research Technical Note NCAR/TN-485+STR, 224 p.

Olson, S.L., Reinhard, C.T., and Lyons, T.W., 2016, Limited role for methane in the mid-Proterozoic greenhouse: National Academy of Sciences Proceedings, v. 113, p. 11,447–11,452, doi:10.1073/pnas.1608549113.

Pavlov, A.A., Hurtgen, M.T., Kasting, J.F., and Arthur, M.A., 2003, Methane-rich Proterozoic atmosphere?: Geology, v. 31, p. 87–90, doi:10.1130/0091-7613(2003)031<0087:MRPA>2.0.CO;2.

Poulsen, C.J., Pierrehumbert, R.T., and Jacob, R.L., 2001, Impact of ocean dynamics on the simulation of the Neoproterozoic "snowball Earth": Geophysical Research Letters, v. 28, p. 1575–1578, doi:10.1029/2000GL012058.

Poulsen, C.J., Tabor, C., and White, J.D., 2015, Long-term climate forcing by atmospheric oxygen concentrations: Science, v. 348, p. 1238–1241, doi:10.1126/science.1260670.

Reinhard, C.T., Planavsky, N.J., Robbins, L.J., Partin, C.A., Gill, B.C., Lalonde, S.V., Bekker, A., Konhauser, K.O., and Lyons, T.W., 2013, Proterozoic ocean redox and biogeochemical stasis: National Academy of Sciences Proceedings, v. 110, p. 5357–5362, doi:10.1073/pnas.1208622110.

Roberson, A.L., Roadt, J., Halevy, I., and Kasting, J.L., 2011, Greenhouse warming by nitrous oxide and methane in the Proterozoic Eon: Geobiology, v. 9, p. 313–320, doi:10.1111/j.1472-4669.2011.00286.x.

Sheldon, N.D., 2006, Precambrian paleosols and atmospheric CO_2 levels: Precambrian Research, v. 147, p. 148–155, doi:10.1016/j.precamres.2006.02.004.

Sheldon, N.D., 2013, Causes and consequences of low atmospheric pCO_2 in the late Mesoproterozoic: Chemical Geology, v. 362, p. 224–231, doi:10.1016/j.chemgeo.2013.09.006.

Som, S.M., Catling, D.C., Harnmeijer, J.P., Polivka, P.M., and Buick, R., 2012, Air density 2.7 billion years ago limited to less than twice modern levels by fossil raindrop imprints: Nature, v. 484, p. 359–362, doi:10.1038/nature10890.

Som, S.M., Buick, R., Hagadorn, J.W., Blake, T.S., Perreault, J.M., Harnmeijer, J.P., and Catling, D.C., 2016, Earth's air pressure 2.7 billion years ago constrained to less than half of modern levels: Nature Geoscience, v. 9, p. 448–451, doi:10.1038/ngeo2713.

Trainer, M.G., Pavlov, A.A., DeWitt, H.L., Jimenez, J.L., McKay, C.P., Toon, O.B., and Tolbert, M.A., 2006, Organic haze on Titan and the early Earth: National Academy of Sciences Proceedings, v. 103, p. 18,035–18,042, doi:10.1073/pnas.0608561103.

Wolf, E.T., and Toon, O.B., 2013, Hospitable Archean climates simulated by a general circulation model: Astrobiology, v. 13, p. 656–673, doi:10.1089/ast.2012.0936.

Manuscript received 11 March 2016
Revised manuscript received 22 November 2016
Manuscript accepted 23 November 2016

Printed in USA